Revista Mexicana de Física **38**, *No. 1 (1992) 40–58*

Equation of state for a small system of hard spheres

DOLORES AYALA DE LONNGI AND PABLO ALEJANDRO LONNGI VILLANUEVA
Areas de Fisicoquímica de Fluidos y Física Estadística, Departamento de Física
Universidad Autónoma Metropolitana, Iztapalapa
Apartado postal 55–534, 09000 México, D.F.

Recibido el 14 de febrero de 1991; aceptado el 14 de agosto de 1991

ABSTRACT. Data for the hard sphere compressibility factor obtained with the discontinuous molecular dynamics (DMD) simulation method are analysed to yield an empirical equation of state. A continued fraction technique is used that allows information on the virial coefficients known from theoretical grounds to be included. This yields irreducible rational functions (IRF), quotient of two quadratic polynomials, independently of the number of DMD data points used. The same kind of IRF is also found for a set of data from other workers. It was possible to fit a rational function, quotient of two quadratics, to a combination of simulation data of different research groups, in good agreement with the result of this work. Implications of this functional dependence on other thermodynamic functions are presented.

PACS: 02.60.+y; 05.70.Ce

1. INTRODUCTION

The hard sphere (HS) system has a very important role as a reference system in the study of fluids. Great effort has been devoted to the knowledge of its properties. In particular, its compressibility factor has been studied by many authors [1,9]. There are some old Molecular Dynamics (MD) and Monte Carlo simulation results as well as more modern and accurate ones, covering the fluid region [10,18]. In Sect. 2 a) we present our own accurate DMD simulation results for the compressibility factor $Z(\rho)$ in the interval $0 < \rho \leq 0.943$.

Expressions for the HS compressibility factor had been reported either constructing Padé approximates [19,26] using its virial coefficients or fitting empirical equations of state to simulation data [14,27]. In this work we incorporate both, virial coefficients and our DMD simulation data, on an equal basis to obtain a simple expression that covers the whole fluid region. This is accomplished by using an approximation procedure, described elsewhere [28], based on Thiele's formula (TF) [29].

The method based on TF and some of its very important features are briefly summarized in 2 b) The Newton-Padé approximates (NPA) obtained for $Z(\rho)$, using TF, are presented in 3, where it is also shown that all the NPA obtained using different sets of tabular data points, either from DMD of from other works, are reducible, through identification of very close roots. In Sect. 4, the cancellation of common

j	ρ	Z_{DMD}	# × 1000
1	0.1	$1.240 \pm 6 \times 10^{-4}$	200
2	0.2	$1.551 \pm 13 \times 10^{-4}$	210
3	0.3	$1.972 \pm 22 \times 10^{-4}$	200
4	0.4	$2.531 \pm 29 \times 10^{-4}$	331
5	0.5	$3.283 \pm 54 \times 10^{-4}$	230
6	0.6	$4.306 \pm 81 \times 10^{-4}$	200
7	0.7	$5.75 \pm 98 \times 10^{-4}$	255
8	0.8	$7.77 \pm 12 \times 10^{-3}$	350
9	0.9	$10.74 \pm 22 \times 10^{-3}$	305
10	0.943	$12.36 \pm 25 \times 10^{-3}$	340

TABLE I. DMD simulation results for the HS compressibility factor with their estimated uncertainties and number of collisions after equilibrium, in thousands. The first column gives the number assigned to each DMD point, used in tables IV and V.

factors is described and the corresponding IRF are reported. In 5 we examine the functional dependence that this result implies for the Helmholtz free energy and the isothermal compressibility of the hard sphere system (derived in Appendix A). Conclusions of this work are discussed in Sect. 6.

2. SIMULATION RESULTS AND METHOD OF ANALYSIS

a) Discontinuous Molecular Dynamics

Results for $Z(\rho)$ and the radial distribution function of a system of $N = 108$ HS of diameter d contained in a volume V, were obtained using the DMD simulation method, described elsewhere [30,31], in the density range $\rho = N/Vd^3$ from 0.1 to 0.9 with increments of 0.1. States with densities $\rho = 0.943$, still on the fluid branch, and 0.95 on the solid branch, were also simulated. The HS DMD results for the compressibility factor are shown in Table I, with the estimated standard deviation of the mean and the number of collisions used after the simulation reached equilibrium.

b) Method of analysis

In order to get a functional representation of $Z(\rho)$ of the HS fluid obtained from the DMD simulation that incorporated the theoretical information contained in the series expansion around $\rho = 0$ through the known HS virial coefficients, Thiele's formula (TF) was used. Since it interpolates at a set of points and satisfies derivative values in a subset of them, TF may be considered as a form of Hermite interpolation giving a continued fraction as a result. From the continued fraction, their successive convergent are rational functions, namely, Newton-Padé approximates (NPA), having

numerator and denominator degrees that depend on the number of points used. Being algorithmic, TF have the advantage of not wasting the effort for building lower order continued fractions. Further details may be found in [28] and references there in. In comparison, the traditional Padé approximates are constructed so as to match just the first coefficients in the power series expansion.

An important characteristic of the TF method is that one can exactly recover an arbitrary rational function (RF) from a tabulation of its values, when these are rational numbers and if rational arithmetic is used in the calculation. If the number of input data (*i.e.*, tabular points and specified derivatives) is greater than the sum of the degrees of the numerator and denominator polynomials (NDP) plus one, there will be redundant data that give no new information. TF will then yield a terminating continued fraction giving an IRF (*i.e.*, with no common factor of degree greater than 0 in NDP) identical to the original.

When TF is applied to tabular values of a known RF perturbed by small deviations, such as rounding errors, it yields a RF with polynomial degrees that depend on the number of data considered. If the number of data points is big enough to overdetermine the function, the resulting RF should be reducible, but any attempt to identify the common factor through the NDP roots will yield very close, but not identical, roots, because of the perturbing effect of the errors in the initial data and, to a lesser extent, of the rounding errors in finding each root. The procedure one uses for dividing them out still perturbs the IRF some more, but the correct functional dependence is recovered, although with coefficients slightly perturbed from their true value. If these effects were nonexistent, the closely lying roots in NDP would be identical and, after cancellation of the common factor, the redundant information would be eliminated.

3. NEWTON-PADÉ APPROXIMATIONS

We applied TF using different combinations of DMD data points and a fixed number of virial coefficients. We decided to include just up to the 5^{th} virial coefficient on the grounds that higher order coefficients have larger relative uncertainties and that they were estimated from fits to specific functional dependence, which might bias somewhat the analysis we are interested in. We chose to use Kratky's "best" values of those virial coefficients [32].

Straightforward application of TF gives, through rationalization of the continued fraction or evaluation of its highest-degree convergent, RF having the degree of numerator equal to either the degree m of denominator or to $m+1$. In the remainder of this work, we shall restrict ourselves just to NPA of the first type, which we denote as $[m/m]$. In order to obtain NPA with its polynomials of the same degree, once decided to include up to the 5^{th} virial coefficient, the maximum number of simulation data points to be considered must be even. When possible, we considered different sets of simulation results as interpolation points.

	Coefficients of ρ^1			
Number of data points n:	12 (EW)		10 (DMD)	
i	Numerator	Denominator	Numerator	Denominator
0	-4.362232×10^{-5}	-4.362232×10^{-5}	-8.672150×10^{-3}	-8.672150×10^{-3}
1	3.601373×10^{-3}	3.692736×10^{-3}	0.1691997	0.1873626
2	-6.050023×10^{-2}	-6.811469×10^{-2}	−1.0567744	−1.4254106
3	4.702050×10^{-2}	0.1796707	2.6129933	5.1075627
4	1.0186781	0.8194745	−2.3419904	−9.6069333
5	−2.3324412	−4.3612297	0.1892669	9.6749239
6	0.4702050	6.9406087	−0.3356989	−4.9182284
7	0.2726582	−4.4407028	0.9299214	1
8	1.7028441	1		

TABLE II. Reducible rational approximates obtained using Thiele's formula and different combinations of simulation data points. The first rational function, [8/8], was obtained from EW's 12 simulation data. The second, [7/7], was obtained from 10 DMD points.

Table II contains the coefficients of the numerator and denominator polynomials for the NPA obtained using Erpenbeck and Wood's (EW) 12 simulation data [14] and the 10 DMD data points of Table I. Table III shows the NPA coefficients obtained from different combinations of 8 and 6 points of our DMD simulation data. Table IV gives the coefficients of the NPA obtained for some combinations of 4 and 2 DMD data points.

A simple graphical analysis of the behaviour of the NPA, as well as of the NPA, as well as of the NDP obtained from different combination of data points, was performed by plotting these three functions simultaneously on the computer screen. We found that whenever the NPA had a singular behaviour in the range $0 < \rho < 1$, it happened around real, very close zeros of its polynomials.

These roots were found using the Bairstow and Newton-Raphson methods [29], in double precision. It was surprising for us to identify that the NPA of Tables II and III have essentially common roots in its polynomials, suggesting, as when dealing with an overdetermined tabulation of a given RF, redundant input data. Table V gives n_r = number of common roots in NDP, the numerator roots of the NPA of higher degree, from [8/8] to [5/5], corresponding to the NPA of Tables II and III, as well as the differences between them and the very close denominator roots.

Indeed, not just the real roots, but also complex conjugate root pairs were found in very close agreement in NDP. The NPA of lower degree contained in Table IV have also very close roots in their polynomials. If, within the accuracy of the simulation data used as input, we accept them to be equal, then the NPA of Tables II, III and IV are reducible, namely, they are equal to IRF having its polynomials of smaller degree.

n	Coefficients of ρ^i						
	i : 0	1	2	3	4	5	6
8	.06737	−.73168	2.27540	−2.31567	.16317	−.19718	.92450
	.06737	−.87278	3.91865	−8.30770	8.97750	−4.77058	1
	.09945	−.90998	2.59446	−2.36878	0.08839	−.36167	0.83870
	0.9945	−1.11827	4.66390	−9.33321	9.58649	−4.89953	1
	.11636	−.98670	2.60093	−2.32656	.16646	−.31902	.90031
	.11636	−1.23040	4.85887	−9.43650	9.60617	−4.90426	1
	.03566	−.53669	1.93599	−2.29039	.19560	−.05931	.96555
	.03566	−.61138	3.11869	−7.24004	8.34513	−4.63156	1
	.02436	−.39199	1.71704	−2.17078	.24950	.04931	.84623
	.02436	−.44301	2.57810	−6.42001	7.74374	−4.46144	1
	.01654	−.29056	1.45215	−2.17839	.28598	.16288	.92724
	.01654	−.32521	2.08792	−5.70335	7.32914	−4.37985	1
6	−.05474	.73646	−1.78578	.68827	.65334	1.00224	
	−.05474	.85112	−3.41827	5.65842	−3.95383	1	
	−.21033	1.40557	−2.14470	.28661	.18596	.89060	
	−.21033	1.84609	−5.43450	7.16192	−4.33545	1	
	−.14759	1.03900	−1.86860	.55492	.45266	.92017	
	−.14759	1.34812	−4.28747	6.22771	−4.07714	1	
	−.02415	.49030	−1.63153	.80770	.76557	.95831	
	−.02415	.54088	−2.69814	5.03948	−3.76663	1	
	−.14457	1.04664	−1.93376	.49035	.40440	.90065	
	−.14457	1.34942	−4.36365	6.31115	−4.10115	1	
	−.03661	.53612	−1.71866	.71636	.68426	.90420	
	−.03661	.61280	−2.90173	5.21023	−3.81056	1	
	−.12101	1.02469	−2.05183	.39666	.35888	.90206	
	−.12101	1.27814	−4.39700	6.42064	−4.14659	1	
	−.02027	1.00731	−2.18575	.29188	.33171	.95376	
	−.02027	1.04976	−4.32878	6.53353	−4.20887	1	

TABLE III. NPA obtained using Thiele's formula, for six different combinations of 8 DMD points and eight combinations of 6 DMD points. In each division the first row gives the numerator and the second row the denominator coefficients of the i-th power of density ρ. The number of DMD points is n.

n	j		Coefficients of ρ^i				
		i :	0	1	2	3	4
4	1,5,	num:	.14593	−1.59949	.87148	.88672	.93886
	8,10	den:	.14593	−1.90513	4.46150	−3.61910	1
	3,5,		.29603	−1.69465	.73616	.74084	.88346
	7,10		.29603	−2.31466	4.77239	−3.68906	1
	2,4,		.25961	−1.42928	.94834	.87336	.88755
	6,10		.25961	−1.97301	4.36887	−3.55205	1
	2,5,		.39661	−1.95366	.50929	.57572	.86301
	8,10		.39661	−2.78431	5.25341	−3.83920	1
	2,5,		.35455	−1.79394	.64002	.66251	.86718
	7,10		.35455	−2.53650	4.98045	−3.74922	1
	3,5		.33754	−1.87020	.59463	.64900	.88089
	8,10		.33754	−2.57714	5.06680	−3.78734	1
	7–10		−.17541	−1.71610	.84781	.97079	.98613
			−.17541	−1.34873	4.15347	−3.56818	1
2	1,10		−.20449	1.94803	1.52559	.92139	
			−.20449	2.37630	−2.89072		
	2,10		−.45609	1.71493	1.36338	.87969	
			−.45609	2.67017	−2.97860	1	
	3,10		−.39682	1.76984	1.40159	.88951	
			−.39682	2.60094	−2.95790	1	
	4,10		−.50602	1.66867	1.33119	.87141	
			−.50602	2.72849	−2.99604	1	
	5,10		−.36339	1.80082	1.42315	.89506	
			−.36339	2.56189	−2.94622	1	
	6,10		1.44454	3.47574	2.58868	1.19473	
			1.44454	.45030	−2.31472	1	
	7,10		.39662	2.50491	1.91311	1.02103	
			.39662	1.67424	−2.68075	1	
	8,10		1.91313	3.90986	2.89077	1.27240	
			1.91313	−.09700	−2.15104	1	
	9,10		−.09240	2.05186	1.59785	.93997	
			−.09240	2.24539	−2.85156	1	

TABLE IV. NPA obtained using Thiele's formula for different combinations of 4 and 2 DMD points. j identifies the points used in each case according to Table I.

n	n_r	j	Roots Numerator r_{num}		Differences $r_{num} - r_{den}$	
12^{EW}	6		4.79129×10^{-2}	1.67349×10^{-2}	-8.5×10^{-7}	5.0×10^{-9}
			-0.234578	0.306029	7.5×10^{-4}	-1.9×10^{-5}
			0.461308	0.613315	-3.2×10^{-5}	-4.0×10^{-5}
10^{DMD}	4	1–10	0.813217	0.207551	-5.5×10^{-5}	-1.0×10^{-5}
			9.78269×10^{-2}		-4.8×10^{-7}	
			$0.497323 \pm i2.635 \times 10^{-2}$		$1.41 \times 10^{-4} \pm i4.46 \times 10^{-5}$	
8^{DMD}	4	3–10	0.811752	0.155484	-4.9×10^{-5}	-7.3×10^{-6}
			$0.500850 \pm i4.199 \times 10^{-2}$		$1.60 \times 10^{-4} \pm i4.47 \times 10^{-5}$	
		2–8, 10	0.217545	0.383057	-2.6×10^{-5}	-1.8×10^{-5}
			0.584615	1.022390	5.0×10^{-5}	3.5×10^{-3}
		2, 4–10	0.224292	0.799644	-4.1×10^{-5}	1.6×10^{-6}
			$0.548697 \pm i9.795 \times 10^{-2}$		$3.12 \times 10^{-4} \pm i6.45 \times 10^{-5}$	
		1,3–5,	9.58809×10^{-2}	0.831046	-8.1×10^{-7}	-1.0×10^{-4}
		7–10	$0.435739 \pm i0.133743$		$-2.5 \times 10^{-5} \pm i2.56 \times 10^{-4}$	
		1, 2, 4–6	0.101662	0.237328	4.5×10^{-7}	-7.2×10^{-5}
		8–10	$0.695352 \pm i0.122179$		$3.4 \times 10^{-4} \pm i(-1.2 \times 10^{-3})$	
		1–4,	9.79154×10^{-2}	0.494692	4.6×10^{-7}	2.7×10^{-4}
		6–7, 10	0.776969	0.207908	-5.7×10^{-5}	-1.1×10^{-5}
6^{DMD}	3	1, 3, 5,	9.55876×10^{-2}		-8.5×10^{-7}	
		6, 8,10	$0.491221 \pm i0.136794$		$2.3 \times 10^{-4} \pm i4.31 \times 10^{-4}$	
		2, 5, 6,	0.221856		-3.5×10^{-5}	
		8–10	$0.669743 \pm i8.908 \times 10^{-2}$		$4.1 \times 10^{-4} \pm i(-6.8 \times 10^{-4})$	
		2, 4, 5,	0.226290		-4.7×10^{-5}	
		7, 9, 10	$0.522289 \pm i0.188638$		$4.3 \times 10^{-4} \pm i2.99 \times 10^{-4}$	
		3, 5, 6,	6.13856×10^{-2}	0.341810	-8.0×10^{-8}	4.5×10^{-5}
		7, 9, 10	0.536378		1.1×10^{-4}	
		2, 5–7	0.224386		-4.2×10^{-5}	
		9, 10	$0.546747 \pm i9.755 \times 10^{-2}$		$3.1 \times 10^{-4} \pm i(-5.9 \times 10^{-5})$	
		1, 3, 5,	9.72551×10^{-2}	0.281648	-5.8×10^{-7}	8.0×10^{-6}
		7, 9, 10	0.633627		1.8×10^{-4}	

TABLE V. Roots of the numerator polynomials and their differences with the roots of the corresponding denominators of the NPA of Tables II and III. n is the number of data points, n_r is the number of common roots and j identifies the points used, according to Table I.

4. IRREDUCIBLE RATIONAL FUNCTIONS

To obtain the IRF, we divided out from the numerator and denominator of the original NPA of Tables II, III and IV the factor associated with those closely lying roots. In this process, however, propagation of small perturbations in the original polynomial coefficients, due to the deviations of the simulation data from the true value, affect the values of the presumably identical roots, in spite of using double precision arithmetic in their evaluation. This, in turn, perturbs the coefficients of the NDP after division. As a result, the IRF thus obtained a) does not necessarily interpolate all data points anymore, b) does not necessarily reproduce exactly the first virial power series expansion coefficients used as input, and c) does not have exactly equal zero-power coefficients in the polynomials suggest that a better the $\rho = 0$ ideal gas limit). These drawbacks suggest that a better procedure is desirable, but the IRF are still very accurate approximates to the tabular data points and the virial coefficients used as input.

The IRF shown in Table VI indeed reproduce the DMD data within their simulation errors and provide estimations of the 2nd virial coefficient B_2 with a percentage difference with respect to its true value smaller than 0.5%, except for a single approximate, for which the maximum difference in B_2 amounts to 1.4%, see last column in Table VI. The last row of Table VI gives the result obtained with our procedure based on TF when exclusively the first five virial coefficients were used, which is in fact a Padé approximate. Here the error quoted for B_2 is entirely due to using the NDP coefficients rounded to six decimal figures.

In addition, due to the fact that the NPA of higher degree have more common roots, as one can see from table V, all the IRF found are the quotient of two quadratic polynomials, of the type which we denote as [2/2], namely,

$$Z(\rho) = \frac{1 + a_1\rho + a_2\rho^2}{1 + b_1\rho + b_2\rho^2}. \tag{1}$$

Since this was unexpectedly simple, we took great efforts to persuade ourselves that the IRF with a form given by Eq. (1) was not a fortuitous result, perhaps dependent on the particular data set taken into account. Thus, the large number of different NPA that we considered, of which those given in Tables II, III and V are but about two thirds of the total. Although only results including the $j = 10$ point are given, the same behaviour was found when using a different end point. Invariably, a quotient of quadratics was obtained after cancelling the factor associated with the closely lying roots.

In order to confirm the generality of that result, we also considered recent data from other workers. In particular, EW's data for 108 particles were chosen because they are accepted to be of high quality. The [8/8] NPA constructed with them also yielded, with this procedure, an irreducible [2/2] rational function shown at the top row of Table VI. This indicates that the equation of state for $Z(\rho)$ has the form

Coefficients of ρ^i for the irreducible rational functions						
Numerator			Denominator			
$i:0$	1	2	0	1	2	$\lvert\%\Delta B_2\rvert$
1.00340	.87444	.63788	1	−1.21019	.37460	.47
.99955	.76913	.43894	1	−1.32411	.47202	.08
.99946	.76773	.43729	1	−1.32531	.47300	.10
.99669	.74368	.41865	1	−1.34544	.49916	.46
.99912	.76110	.43073	1	−1.33171	.47843	.13
.99991	.77845	.44816	1	−1.31494	.46415	.05
.99992	.74696	.41777	1	−1.34892	.49369	.07
.99959	.76849	.43835	1	−1.32490	.47275	.07
.99869	.78611	.45442	1	−1.30412	.45341	.28
.99924	.75850	.42850	1	−1.33509	.48113	.09
.99838	.76566	.43434	1	−1.32502	.47203	.28
.99967	.77619	.44649	1	−1.31722	.46591	.05
.99912	.76119	.43081	1	−1.33160	.47833	.05
.99975	.76778	.43800	1	−1.32614	.47393	.04
.99970	.76206	.43206	1	−1.33198	.47897	.04
.99989	.77509	.44617	1	−1.31898	.46780	.02
.99930	.77104	.44086	1	−1.32187	.46957	.07
1.00035	.75775	.42841	1	−1.33773	.48492	.07
.99982	.75835	.42859	1	−1.33605	.48289	.01
1.00068	.75271	.42437	1	−1.34344	.49173	.13
1.00085	.75383	.42508	1	−1.34273	.49019	.16
1.00041	.75717	.42799	1	−1.33840	.48586	.08
1.00013	.78202	.45609	1	−1.31255	.46250	.02
1.00001	.76730	.43773	1	−1.32717	.47508	4×10^{-3}
1.00015	.75653	.42712	1	−1.33868	.48553	.05
1.00009	.75912	.42954	1	−1.33581	.48289	.03
1.00023	.75434	.42512	1	−1.34118	.48785	.07
1.00006	.76566	.43093	1	−1.33423	.48145	.02
1.01339	.80374	.51961	1	−1.27997	.43492	.31
1.00009	.78849	.46579	1	−1.30550	.45620	.01
1.03594	.80692	.54475	1	−1.27160	.42813	1.4
1.00000	.77184	.44272	1	−1.32256	.47099	3×10^{-4}
1.00000	.69864	.38663	1	−1.39576	.56834	2×10^{-7}

TABLE VI. Numerator and denominator coefficients of the IRF obtained from Tables II, III and IV. The last column contains the percentage uncertainties of B_2 when estimated from the IRF.

given by Eq. (1) independently of the particular simulation data points used as input.

As a further test of the NPA and of their irreducible form, we evaluated their virial (power series) coefficients, using an algorithm similar to the one described by Ree and Hoover [8], of which the latter is an special case. Except for small changes in the least significant digits attributable to rounding errors in the calculations, the reducible NPA reproduced, as they should, up to the 5^{th} virial coefficient, but invariably gave wild estimations of the higher order coefficients.

A little thought makes the reason for this clear. The recurrence relation (RR) of the algorithm is, for the higher order coefficients, a difference equation that has as characteristic polynomial the denominator polynomial but with its coefficients in the reverse order. From elementary algebra, the characteristic polynomial roots are the reciprocal of the denominator roots, and thus the general solution of the RR contains terms proportional to the n^{th} power of the reciprocal of the roots in Table V. Since they are all smaller than unity in absolute value, their contribution to the general solution of the difference equation make the application of the RR unstable.

On the other hand, application of the RR for the IRF is stable and all the equations of Table VI provide values of the first eight virial coefficients with relative deviations lower than 7%, when compared with Kratky's values, in spite that just up to the fifth virial coefficient, in addition to the tabular points, were used as input. This suggest that the roots in Table 5 should be considered as superfluous, as we did when cancelling factors due to the closely lying roots in reconstructing a RF from tabular data with rounding errors, and therefore, that Table VI may be regarded as evidence that the HS compressibility factor is an IRF such as Eq. (1). Notice that the first and last lines of Table VI give extreme values for the coefficients of the quadratics, but most IRF are within a much sharper range.

The conjecture that $Z(\rho)$ is of the form (1) was tested using a different procedure with a combination of EW's and our simulation data (EWDMD). Now, we postulated Eq. (1) satisfying the constraints: 1) equal zeroth power coefficients and 2) exact 2^{nd} and 3^{rd} virial coefficients, B_2 and B_3. We then fitted the coefficients in the quadratics for vanishing sum of deviations, minimum sum of absolute deviations, least squares and minimax [29] approximations to EWDMD, separately. It was found that those criteria give coefficients that differ only slightly, but all are consistent with equation

$$Z^{\mathrm{HS}}_{\mathrm{EWDMD}} = \frac{1 + 0.781844\rho + 0.455061\rho^2}{1 - 1.312551\rho + 0.462505\rho^2} \tag{2}$$

within the number of decimal figures quoted.

In spite of its simplicity, Eq. (2) produces smaller overall residuals in the whole fluid range ($0 \leq \rho \leq 0.943$), when compared with EWDMD simulation data, than the very good equations set forth by Erpenbeck and Wood [14], of degrees [4/2],

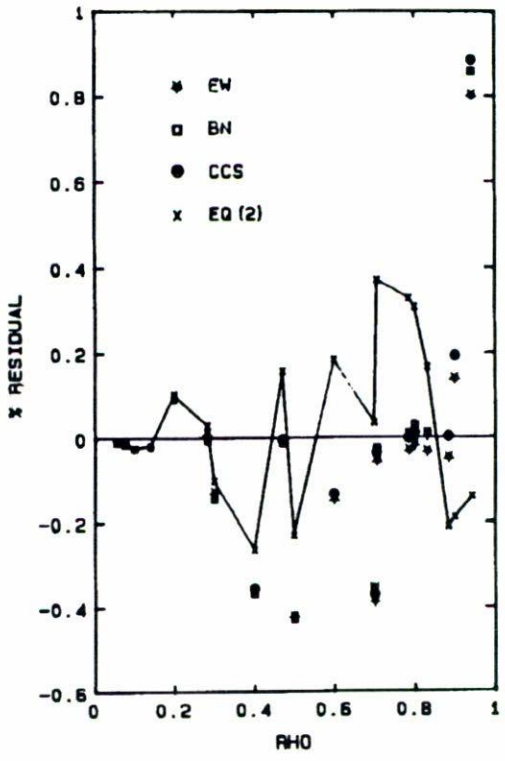

FIGURE 1. Percentage residuals of several equations of state for the HS compressibility factor with respect to simulation data from Table VII: (∗) EW, (□) BN, (+) CCS and (×) Eq. (1) of this work.

Boublick and Nezbeda (BN) of degrees [5/3] and the so-called corrected Carnahan-Starling (CCS) [27] of degrees [4/3], see Table VII. Figure 1 shows the percentage residuals for all four equations with respect to the EWDMD simulation data. We can see that all of them offer good accuracy at low densities. EW, BN and CCS tend to yield a very good fit at particular values of density, while giving a large residual at others, such as 0.5 and 0.943. In comparison, Eq. (2) gives more uniformly distributed residuals. Its power series expansion gives estimates of the 4^{th} up to the 8^{th} virial coefficients given in Table VIII, with relative errors of .24%, 2.9%, 5.3%, .05% and 5.2% with respect to Kratky's values. In particular, even the value obtained for B_8 is well within the suggested bounds of 0.0042 B_2^7 to 0.0052 B_2^7. In [33] we give estimates of higher order virial coefficients associated with Eq. (2).

We would like to stress that Eq. (2) was obtained using a fitting procedure for the EWDMD combined set of simulation data and that it provides excellent results in comparison with the very best equations of state available. It is worth mentioning that values of the coefficients in NDP of Eq. (2), are contained in the interval defined in Table VI.

		Residuals %			
ρ	Z	EW	BN	CCS	Eq. 2
0.0565†	1.1278	−.010	−.010	−.010	−.010
0.0785†	1.1828	−.014	−.015	−.014	−.014
0.1 *	1.2400	−.024	−.026	−.025	−.024
0.1413†	1.3594	−.018	−.021	−.019	−.017
0.2 *	1.5521	.098	.092	.097	.103
2.2829†	1.8884	.005	−.006	.004	.029
0.3 *	1.9708	−.132	−.144	−.133	−.102
0.4 *	2.5306	−.355	−.368	−.354	−.265
0.4714†	3.0311	−.003	−.011	.001	.157
0.5 *	3.2833	−.424	−.429	−.419	−.231
0.6 *	4.3010	−.142	−.132	−.131	.183
0.7 *	5.7485	−.384	−.356	−.366	.036
0.7070†	5.8502	−.053	−.024	−.036	.370
0.7857†	7.4304	−.030	.011	−.005	.327
0.8 *	7.7689	−.012	.030	.014	.307
0.8319†	8.6003	−.031	.014	.000	.165
0.8839†	10.1939	−.045	.003	−.001	−.211
0.9 *	10.7390	.141	.191	.193	−.190
0.943 *	12.3595	.802	.858	.880	−.140
(*EW, †DMD)					
Sum of residuals:		.048	.078	.077	.024
Average mod. res:		.0092	.0094	.0094	.0089
Standard dev:		.023	.025	.025	.012

TABLE VII. Percentage residuals of various HS equations of state with respect to simulation results from EW and DMD. a) EW, b) BN c) CCS and d) equation (2) of this work. The last three rows show the sum of residuals, the average of the absolute value of the residuals and the sum of their standard deviations, respectively.

i	4	5	6	7	8
$\frac{B_i}{B_2^{i-1}}$	0.286247	0.113491	0.040943	0.013693	0.004264

TABLE VIII. Estimations, to six decimal digits, of the virial coefficients 4^{th} to 8^{th} from Eq. (2).

Another interesting aspect is that other equations, such as Ree-Hoover's [8] and Erpenbeck-Wood's, derived with different procedures and from different points of view, predict a quadratic polynomial denominator too.

It is worthwhile mentioning that, in the analysis of DMD data for the compressibility factor of square well systems with elongations $R/d = 1.4$ and 1.6, in the high temperature limit and up to relatively low reduced temperatures ($T = 4$), the

same kind of functional dependence was found [30], in agreement with these results. We consider this as additional evidence that the true HS equation of state for a HS system of 108 particles is of the form given in (1).

Further, since Eq. (2) should be subjected to extensive testing, we would like to suggest that the functional dependence that it implies for the Helmholtz free energy and for the isothermal compressibility should also be considered. Therefore, in the following section we give the corresponding expressions for these functions derived from Eq. (2).

5. HELMHOLTZ FREE ENERGY AND ISOTHERMAL COMPRESSIBILITY

In terms of the packing fraction $\eta = (\pi/6)\rho$, Eq. (2) is equivalent to

$$Z(\eta) \simeq \frac{1 + 1.493212\eta + 1.659864\eta^2}{1 - 2.506788\eta + 1.687016\eta^2} \tag{3}$$

The general form for the Helmholtz free energy and the isothermal compressibility associated with Eq. (1) were derived in the Appendix. In terms of η and according to Eqs. (A5) and (A9) of the appendix, the excess free energy per particle and the isothermal compressibility are given, respectively, by

$$\beta\Delta a_e = \ln[g^{-0.008047}] + 11.6842\tan^{-1}[4.95284\eta - 3.67978] \tag{4}$$

and

$$\frac{\rho}{\beta}K_T = \frac{g^2}{1 + 2.98642\eta - .45059\eta^2 - 8.32185\eta^3 + 2.80022\eta^4}, \tag{5}$$

where g is the denominator of Eq. (3).

For practical purposes we approximated the coefficients of Eq. (3) to the simplest closest rational numbers, as follows:

$$Z(\eta)^{\text{app}} \simeq \frac{1 + \frac{3}{2}\eta + \frac{5}{3}\eta^2}{1 - \frac{5}{2}\eta + \frac{27}{16}\eta^2}. \tag{3'}$$

Similarly, Eqs. (4) and (5) can be written as

$$\beta\Delta a_e^{\text{app}} \simeq \ln(g^{\gamma}) + \frac{1291}{81\sqrt{2}}\tan^{-1}\left[\frac{27}{4\sqrt{2}}\eta - \frac{5}{\sqrt{2}}\right] \tag{4'}$$

and

$$\frac{\rho K_T^{\text{app}}}{\beta} \simeq \frac{g^2}{1 + 3\eta - \frac{5}{16}\eta^2 - \frac{25}{3}\eta^3 + \frac{45}{16}\eta^4}, \tag{5'}$$

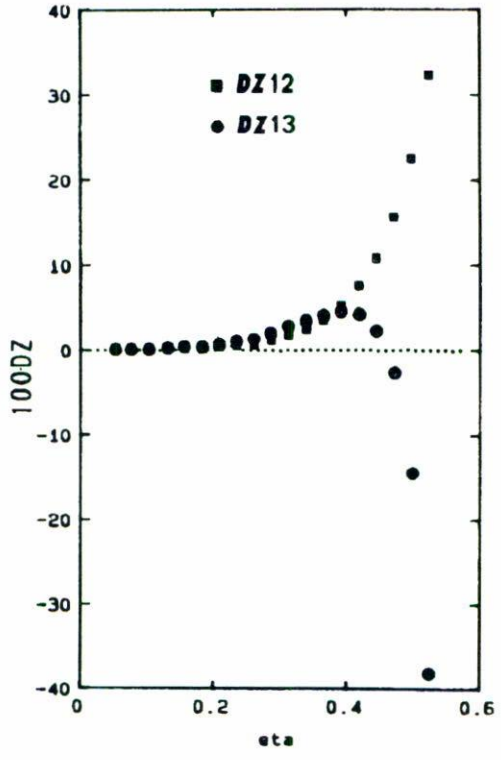

FIGURE 2. Differences of CS and approximate expression for the compressibility factor with respect to Eq. (3). (■) represent $100 \times Z_{12} = 100 \times [(3) - (3')]$ and circles are $100 \times Z_{13} = 100 \times [(3) - Z_{CS}]$.

where g is now the denominator of Eq. (3′) and γ turns out to be $-1/162 = -0.006173$. However, this approximate γ is quite different from its exact value $\gamma = -0.008047 = -1/124.26$, and therefore, we suggest to approximate it by $-1/124$.

Differences between the values predicted by Eq. (3) and the approximate Eq. (3′), represented as $Z_{12} = (3) - (3')$, and with Carnahan-Starling (CS) expression [19], $Z_{13} = (3) - Z_{CS'}$ were calculated and they are shown as DZ in Fig. 2. One can see that at low η, Z_{12} and Z_{13} are almost zero and that they start growing together, from $\eta \geq 0.25$, up to a value less than 0.05 at $\eta \leq 0.4$. For $\eta \geq 0.4$ CS predicts values greater than (3) while Eq. (3′) predicts values lower than the exact equation.

Now we analyse the effect of these deviations on the Helmholtz free energy and the isothermal compressibility. The differences between the exact, Eq. (4), and the approximate Eq. (4′), represented by Δa_{12}, and with CS expression, represented as Δa_{13}, for the excess Helmholtz free energy were calculated and represented as Da in Fig. 3(a), where one can observe that, for $\eta \leq 0.2$, Δa_{12} is slightly lower than cero and starts increasing with density, reaching a value of 0.05 at $\eta = 0.52$. On

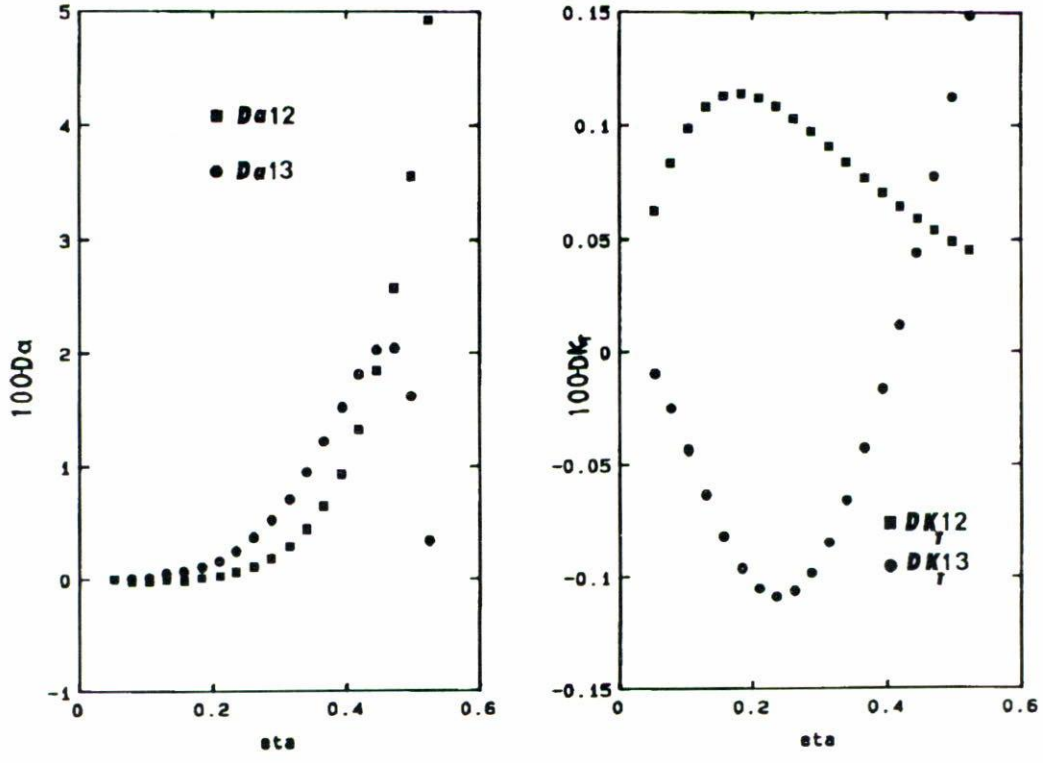

FIGURE 3. Difference of CS (o) and approximate expressions (■) for: (a) the change in Helmholtz free energy, Eq. (4′) with respect to Eq. (4), and (b) the isothermal compressibility, Eq. (5′) with respect to Eq. (5).

the other hand, Δa_{13} is negligible up to $\eta = 0.1$ and has a maximum of 0.02 at $\eta = 0.45$ where it decreases quickly up to 0.003 at $\eta = 0.52$.

Differences DK_T between the exact, Eq. (5), and the approximate expression, Eq. (5′), K_T12, and with CS expression, K_T13 are shown in Fig. 3(b). K_T12 is positive reaching a maximum of 0.12×10^{-2} at $\eta < 0.2$ and decreasing slowly as η increases. K_T13 is negative and presents a minimum of 0.11×10^{-2} at $\eta = 0.24$, where it starts to increase with η.

The smallness of the differences Dz, Da and DK_T between Eq. (3) and the corresponding CS expressions, shown in Figs. 2 and 3, provide additional evidence of the appropriateness of Eq. (2).

6. CONCLUSION

In this work we found an empirical equation of state for the HS system that has the form of a quotient of quadratic polynomials. The method that we applied

goes beyond the Padé approximate concept and handles both theoretical (power series coefficients) and experimental (simulation) data on an equal basis. For an interpolative method, it has the remarkable capability of dealing correctly with overdetermination in the supplied data, even in the presence of uncertainties in the input data.

The NPA first obtained by means of this method have closely lying roots that are superfluous. If not eliminated, superfluous roots give rise to incorrect, rapidly growing, high order power series coefficients. Since they would be identical in absence of uncertainties of the input data and rounding errors, they indicate reducibility of those NPA.

The IRF that we obtained after dividing out the factor associated with the closely lying roots becomes just an approximate solution to the original interpolation problem. However, from the point of view of backward error analysis, it is the exact solution to a problem that differs slightly from the original.

The very definite ranges for the coefficients in the IRF obtained after this division, points to the good conditioning of the procedure. On the grounds that different selections of simulation points yielded IRF which are invariably quotients of quadratic polynomials, we advance the conjecture that the equation of state of a HS system is indeed given by a RF of this kind, with coefficients that should not be very different from those given in (2). This equation of state reproduces the virial coefficients B_2 and B_3 exactly and B_4 to B_8 to within a few percent.

The expressions for other thermodynamic functions, such as the Helmholtz free energy and the isothermal compressibility derived from the empirical equation for Z obtained in this work, clearly support its consistency as a good equation of state.

The accuracy of the simulation data, the density range covering the full fluid region and the appropriateness of the procedure of analysis led us to find that the HS compressibility factor for the small system of 108 particles, is well described by a quadratic RF.

In fact, in a recent paper [34] we found that, for a larger system of 4000 HS particles, the equation of state is an irreducible rational function quotient of cubic polynomials. These result allow us to say that the equation of state of the HS fluid is a rational function quotient of polynomials of degrees not greater than 3.

APPENDIX A

We found above that the equation of state of the HS fluid,

$$Z(\rho) = \frac{\beta P}{\rho}, \tag{A1}$$

has the general form of Eq. (1), where $\beta = 1/(kT)$, with k Boltzmann's constant, T the absolute temperature and P the pressure of the system. P can be expressed

in terms of the Helmholtz free energy as

$$P = \rho^2 \left(\frac{\partial a}{\partial \rho}\right)_T, \tag{A2}$$

where α is the free energy per particle. Then, integrating at constant temperature from a reference state to an arbitrary state,

$$a = \int \frac{P}{\rho^2}\, d\rho = \frac{1}{\beta} \int \frac{Z}{\rho}\, d\rho \tag{A3}$$

and

$$\beta a = \int \frac{1 + a_1\rho + a_2\rho^2}{\rho(1 + b_1\rho + b_2\rho^2)}\, d\rho. \tag{A4}$$

Assuming $4b_2 > b_1^2$, the Helmholtz free energy per particle of the HS system is thus given by

$$\beta \Delta a = \ln[\rho g^\gamma] + \frac{f}{\delta} \tan^{-1} \frac{b_1 + 2b_2\rho}{\delta}, \tag{A5}$$

with

$$g = 1 + b_1\rho + b_2\rho^2, \qquad \gamma = \frac{a_2 - b_2}{2b_2}, \tag{A6}$$

$$f = 2a_1 - b_1 - \frac{a_2 b_1}{b_2} \qquad \text{and} \qquad \delta = \sqrt{4b_2 - b_1^2}. \tag{A7}$$

Now we turn to the isothermal compressibility K_T, which is given by

$$\frac{K_T}{\beta} = \frac{1}{\rho} \left(\frac{\partial \rho}{\partial P}\right)_T. \tag{A8}$$

Then, from Eq. (3), the isothermal compressibility of the HS system is given by

$$\frac{K_T}{\beta} = \frac{(1 + b_1\rho + b_2\rho^2)^2}{\rho\left[1 + 2a_1\rho + (3a_2 - b_2 + b_1 a_1)\rho^2 + 2a_2 b_1 \rho^3 + a_2 b_2 \rho^4\right]}. \tag{A9}$$

These two functions can be evaluated and compared with results obtained using different approaches, as a further test of the equation of state found in this work.

REFERENCES

1. Wertheim M., *Phys. Rev. Lett.* **10** (1963) 321.
2. Thiele E., *J. Chem. Phys.* **39** (1963) 474.
3. Smith W.R. and Henderson D., *Mol. Phys.* **19** (1970) 411.
4. Watts R.O. and Henderson D., *Mol. Phys.* **16** (1969) 217.
5. Barker J.A. and Henderson D., *J. Chem. Phys.* **47** (1967) 2856, 4714.
6. Weeks J.D., Chandler D. and Andersen H.C., *J. Chem. Phys.* **54** (1971) 5237.
7. De Lonngi D.A. and del Río F., *Mol. Phys.* **42** (1983) 293; **56** (1985) 691.
8. Ree F.H. and Hoover W.G., *J. Chem. Phys.* **40** (1964) 939.
9. Speedy R.J., *J. Chem. Soc., Faraday Trans. 2,* **73** (1977) 714; *J. Chem. Soc., Faraday Trans.* **75** (1979) 1643.
10. Alder B.J. and Wainwright T.E., *J. Chem. Phys.* **31** (1959) 459.
11. Barker J.A. and Henderson D., *Mol. Phys.* **21** (1971) 187.
12. Verlet L. and Weis J.J., *Phys. Rev. A,* **5** (1971) 939; *Mol. Phys.* **24** (1972) 1013.
13. Labik S. and Malijevsky A., *Mol. Phys.* **42** (1982) 739.
14. Erpenbeck J.J. and Wood W.W., *J. Stat. Phys.* **35** (1984) 321.
15. Groot R.D., van del Ferden J.P. and Faber N.M., *J. Chem. Phys.* **87** (1987) 15.
16. Labik S. and Malijevsky A., *Czech. J. Phys. B* **33** (1983) 128.
17. Nezbeda I., Labik S. and Malijevsky A., *Collect. Czech. Commun.* **54** (1989) 1145.
18. Adams, D.J., *Mol. Phys.* **28** (1974) 1241.
19. Carnahan N.F. and Starling K.E., *J. Chem. Phys.* **51** (1969) 635.
20. Hoover W.G. and Ree F.H., *J. Chem. Phys.* **47** (1967) 4873; *J. Chem. Phys.* **49** (1968) 3609.
21. Devore J.A. and Scheider E., *J. Chem. Phys.* **77** (1982) 1067.
22. Hall K.R., *J. Chem. Phys.* **57** (1972) 2252.
23. Le Fevre E.J., *Nature* **20** (1972) 235.
24. Woodcock L.V., *J. Chem. Soc., Faraday Trans.* **II 72** (1976) 731.
25. Hoste R. and Van Dael W., *J. Chem. Soc. Faraday Trans.* **2**, 80 (1984) 477.
26. Baker G. jr., Gutierrez G. and de Llano, M., *J. Chem. Phys.* **153** (1984) 283.
27. Boublik T. and Nezbeda I., *Collection Czechoslovak Chem. Commun.* **51** (1986) 2342, 2356 and 2357.
28. Longgi P.A. and de Longgi D.A., "Methods for Representing Physical Properties through Rational Approximates". to be submitted to *J. Math. Phys.*
29. Ralston A., *A first Course in Numerical Analysis,* McGraw-Hill New York (1965).
30. De Lonnggi, D.A., Lonngi P.A. and Alejandre J., "The square well fluid: Its properties and representation. I Compressibility factor". *Mol. Phys.* **72**, 2, (1990) 427.
31. Chapela G.A., Martinez-Casas S.E. and Alejandre J., *Mol. Phys.* **53** (1984) 139.
32. Kratky K.W., *Physica* **87A** (1977) 588.
33. De Lonngi D.A. and Lonngi P.A., "A Direct Approach to Padé Approximates. Virial Convergent for Hard Spheres", to be submitted.
34. De Lonngi D.A. and Lonngi P.A., "Irreducible Rational Approximates for the hard sphere fluid", to appear in *Mol. Phys.* (1991).

RESUMEN. Se analizaron datos del factor de compresibilidad obtenidos con el método de simulación de dinámica molecular discontinua (DMD) a fin de obtener una ecuación de estado empírica. Se usó en el análisis una técnica de fracción continua que permite incluir la información conocida teóricamente acerca de los coeficientes viriales. Esto produjo funciones racionales irreducibles que son cociente de dos polinomios cuadráticos independientemente del número de datos de DMD usados. Se encontró el mismo tipo de función racional irreducible para datos de otros investigadores. Se pudo ajustar una función racional, cociente de dos polinomios cuadráticos, a una combinación de datos de simulación de diferentes investigadores, en concordancia con el resultado obtenido en este trabajo. Se presentan las implicaciones de este resultado en otras funciones termodinámicas.